THE ASTROPHYSICAL JOURNAL, 557:736–746, 2001 August 20

MOLECULAR DEPLETION AND THERMAL BALANCE IN DARK CLOUD CORES

PAUL F. GOLDSMITH
National Astronomy and Ionosphere Center, Department of Astronomy, 512 Space Sciences Building, Cornell University, Ithaca, NY 14853; pfg@astrosun.tn.cornell.edu
Received 2001 January 15; accepted 2001 April 19

ABSTRACT

We analyze the effects of molecular depletion on the thermal balance of well-shielded, quiescent dark cloud cores. Recent observations of the significant depletion of molecules from the gas phase onto grain surfaces in dark clouds suggest the possibility that the gas-phase cooling in these regions is greatly reduced and consequently that gas kinetic temperatures might be increased. We reexamine cooling and heating processes in light of possible molecular depletion, including the effect of coupling between the gas and the grains. At densities $\lesssim 10^{3.5}$ cm^{-3}, the gas temperature can be significantly increased by the depletion of coolant species without significantly affecting the dust temperature because of the relatively weak gas-dust coupling. At higher densities, this coupling becomes sufficiently rapid to overwhelm the effect of the reduced gas-phase cooling, and depletion has little effect on the gas temperature while raising the dust temperature $\simeq 1$ K. The result is that depletion at densities $\gtrsim 10^{4.5}$ cm^{-3} can proceed without being evident as an enhanced gas temperature or without self-limiting due to an increase in the dust temperature increasing the desorption rate. This is consistent with observations of depletion in cold, dense regions of quiescent molecular clouds. It also suggests that depletion in moderate density regions can increase the thermal gas pressure, effectively enhancing the confinement of denser portions of molecular clouds and possibly accelerating the collapse of cloud cores.

Subject headings: ISM: clouds — ISM: globules — ISM: molecules — molecular processes

1. INTRODUCTION

Molecules and dust are the dominant forms of mass in well-shielded regions in the Milky Way and other galaxies. Since the most abundant molecular species, H_2, does not readily emit radiation at the low temperatures characterizing quiescent clouds, relatively rare polar species such as carbon monoxide, carbon monosulfide, ammonia, and others are the dominant coolants of the gas phase and also serve as probes of the kinematics and physical conditions of these regions. Their cooling and tracing of the gas depend on their abundances, which are not straightforward to determine. One way of assessing molecular abundances relative to that of dust is to trace the gas column density using a nonselective molecular species and to employ the visible or near-infrared extinction to measure the dust. While initial investigations showed plausibly good correlation between the two, once an initial threshold at low column densities is achieved (Frerking, Langer, & Wilson 1982), more extensive investigations have suggested that this correlation breaks down at very large column densities, suggestive of the depletion of molecules from the gas phase onto dust grains (Kramer et al. 1999).

Both gas and dust column densities have associated uncertainties that become more severe when one probes complex regions with embedded energy sources producing significant variations in conditions along the line of sight. Despite these problems, studies of cold, star-forming condensations have been interpreted as indicating significant depletion of molecules from the gas phase (Mauersberger et al. 1992; Carey et al. 1998; Visser et al. 1998; Gibb & Little 1998). The plausibility of a major reduction in the abundance of particular species in the central regions of clouds is reinforced by peculiar morphologies seen in the maps of some species; there appears to be a deficiency of emission from certain molecules in the cores of the clouds observed (Kuiper, Langer, & Velusamy 1996; Willacy, Langer, & Velusamy 1998b; Caselli et al. 1999; Ohashi et al. 1999).

From a theoretical point of view, it is not surprising that there should be an appreciable depletion of gas-phase molecules onto dust grain surfaces. Broadly speaking, gas-phase molecules will collide with and stick to the surface of a dust grain, with a characteristic timescale[1] $t_{acc} = 10^9$ yr $[n(H_2)]^{-1}$. At densities of 10^3–10^5 cm^{-3} characteristic of dark cloud cores, the depletion timescale is sufficiently short that a large fraction of the gas phase could be trapped on the surface of the dust grains. This effect is seen in a number of theoretical studies that include the dust grains along with gas-phase chemistry (e.g., Brown, Charnley, & Millar 1988; Willacy & Williams 1993; Hasegawa, Herbst, & Leung 1992; Hasegawa & Herbst 1993; Bergin, Langer, & Goldsmith 1995). There is considerable uncertainty regarding the efficacy of various potential desorption processes (Léger, Jura, & Omont 1985; Dzegilenko & Herbst 1995; Willacy et al. 1998a). The uncertainty (or at least differences between different compilations) in the binding energy of adsorbed molecules on the grain surfaces contributes significantly to the uncertainties in the rate of various desorption processes (Léger et al. 1985; Hasegawa et al. 1992; Hasegawa & Herbst 1993; Aikawa et al. 1997; Willacy et al. 1998a).

There is also increasing direct observational evidence that a variety of molecular species are bound on the surface of dust grains (see, e.g., Tielens & Whittet 1997). Most of these results come from infrared spectroscopy, and the *Infrared Space Observatory* has significantly expanded this data (see, e.g., Gibb et al. 2000). It is quite difficult to know exactly how the column densities or abundances of species

[1] This assumes a sticking coefficient of unity, standard dust grain parameters, and a dust-to-gas ratio of 100 by mass.

observed on dust grain surfaces are related to the abundances in the gas phase, particularly because the chemical reactions that molecules on grain surfaces may undergo can lead to the release of molecules (generally different species than the reactants) back to the gas phase.

If kinematic tracers are disappearing from the gas phase in the central regions of dark cloud cores, it will make studying the evolution of these regions extremely difficult. If major fractions of gas-phase coolants are depleted, the thermal balance within these regions will certainly be changed. These plausible effects make a reexamination of dark cloud thermal balance in the context of molecular depletion appropriate at this time.

2. MOLECULAR ABUNDANCES AND GAS COOLING

2.1. *Standard Abundances and Collisional Excitation Data*

The various isotopic variants of the carbon monoxide molecule are certainly important coolants of dark clouds. The abundance of ^{12}CO has been measured directly by infrared absorption (Lacy et al. 1994). The less abundant variants can be probed by their millimeter-wavelength emission, and the estimates of their abundances are fairly consistent with the common isotopic species and the isotopic abundance ratio (see discussion in Goldsmith, Bergin, & Lis 1997). Based on these data, we adopt the "standard" abundances for ^{12}CO, ^{13}CO, and $C^{18}O$ given in Table 1. We have used the cross sections for CO-H_2 collisions of Flower & Launay (1985) extrapolated to include the lowest 20 CO rotational levels. The collision rate coefficients depend on the symmetry state of the H_2 collision partners, with the deexcitation rates for ortho-H_2 being approximately twice those for para-H_2 at cloud temperatures between 10 and 40 K. This difference is reflected in the cooling rate only at low densities when the excitation temperatures of relevant (low J for the kinetic temperatures in question) transitions are subthermal. The dependence of the cooling rate Λ on the ortho-to-para ratio (o/p) of H_2 is comparable to the difference between the cross sections calculated by Flower & Launay (1985) and other quantum calculations (Schinke et al. 1985). We thus adopt an H_2 o/p = 0.5, which is a compromise value in terms of the cooling rate. This does not produce an appreciable increase in the uncertainty in the gas cooling rate.

Observations using the *Submillimeter Wave Astronomy Satellite* (*SWAS*) have revealed that even in fairly warm ($T_{\rm kinetic} \geq 30$ K), relatively quiescent regions of giant molecular clouds (GMCs), the fractional abundance of water vapor is surprisingly low: $X(H_2O) = 10^{-9}$ to 10^{-7}(Snell et al. 2000a, 2000b, 2000c; Ashby et al. 2000). The abundance in colder, even less turbulent central regions of dark clouds could well be significantly less, but these regions are not easily probed by the transition available to *SWAS*. We adopt a fractional abundance for ortho-H_2O equal to 10^{-8}, as given in Table 1. Molecular oxygen also appears to be significantly underabundant in GMCs compared to predictions of steady state chemical models; the upper limits for $N(O_2)/N(H_2)$ are between 10^{-7} and 10^{-8} (Goldsmith et al. 2000). Although the situation in cold, dark clouds is not as highly constrained, O_2 at these abundance levels would not be a significant coolant and is not specifically included in our calculations.

TABLE 1

UNDEPLETED STANDARD FRACTIONAL ABUNDANCES OF COOLANT SPECIES

Species	Fractional Abundance[a]	Multiplier
^{12}CO	5.62×10^{-5}	1.0
^{13}CO	1.00×10^{-6}	1.0
$C^{18}O$	1.00×10^{-7}	1.0
C	1.00×10^{-6}	1.0
o-H_2O	1.00×10^{-8}	2.0
$^{12}C^{32}S$	3.16×10^{-8}	10.0
O	1.00×10^{-6}	1.0

[a] Number density of each species relative to that of H_2.

The water cooling calculation is carried out for ortho-H_2O using the collisional cross sections calculated by Phillips, Maluendes, & Green (1996). For general use, the deexcitation cross sections obtained from this work were extrapolated to include the 25 lowest levels of ortho-H_2O. The collision rates for ortho-H_2O with H_2 in the $J = 0$ state (para-H_2) are significantly less than those with H_2 in states having $J \geq 1$ (essentially ortho-H_2 at moderately low temperatures) according to Phillips et al. (1996). The $J = 1$ level (the lowest level of ortho-H_2) lies approximately 171 K above the $J = 0$ level (the lowest level of para-H_2). In consequence, the LTE ratio of ortho to para-H_2 at dark cloud temperatures will be extremely small, but the observational situation suggests that the o/p for H_2 (in warmer regions) is significantly different from the LTE value and not very far from unity (see, e.g., Hoban et al. 1991; Lacy et al. 1994; Neufeld, Melnick, & Harwit 1998). We have adopted a fraction of the H_2 in $J = 0$ equal to 0.5; this may somewhat overestimate the contribution of H_2O to the total cooling rate. We have also doubled the ortho-H_2 cooling rate to account approximately for the contribution of para-H_2, but for the low fractional abundance of H_2O indicated by *SWAS*, the contribution of water to the total cooling is not very significant.

There is a large number of molecular species, including CN, HCN, CS, NH_3, HCO^+, and H_2CO, that have fractional abundances of approximately 10^{-8} in dark clouds (Ohishi, Irvine, & Kaifu 1992). To simplify the cooling calculation, we adopt the CS molecule as representative and multiply its cooling by a factor of 10 to include the contribution of the other species in this category. We have used the collisional cross sections calculated by Green & Chapman (1978) for collisions between CS and H_2, extrapolating their results from 13 to 25 levels of the CS molecule.[2]

Neutral carbon (C) is an important coolant since although it has only two fine structure transitions available, they have modest energies, and the abundance of this atom is relatively large. We have used the collision rates of Schröder et al. (1991), which treat ortho- and para-H_2 separately. In this case, the differences are less than a factor of 2, so that assuming an o/p for H_2 introduces only a relatively minor uncertainty. The fractional abundance of C is highly dependent on extinction, and measurement necessarily blend regions along the line of sight. We have thus extrapolated the dependence found by Frerking et al. (1989)

[2] The referee pointed out the quantum calculations of the collisional excitation of CS by Turner et al. (1992), which include levels up to $J = 20$. These do not differ significantly from the extrapolated rates used here, and given that levels above $J = 12$ contribute only a few percent to the cooling for temperatures ≤ 30 K and for densities $\leq 10^6$ cm^{-3}, the present cooling rates appear to be satisfactory.

to the relatively small value given in Table 1. However, even this small value may be an overestimate for an evolved, well-shielded dark cloud core (see, e.g., Schilke et al. 1995). We do not, however, consider further depletion of the abundance of atomic carbon.

At the very low temperatures of interest in the well-shielded regions of dark clouds, many generally important coolants do not play a significant role because of the absence of low-lying energy levels. Notable in this category are H_2, HD, and other hydrides, and in this study we neglect their contribution to the gas cooling. Atomic oxygen is relatively inefficient as a coolant at dark cloud temperatures because of the large spacing of its fine structure levels. Its abundance is extremely uncertain; although there are some cases in which this species is claimed to contain almost all available oxygen atoms (see, e.g., Caux et al. 1999), it is not at all certain what the abundance is in well-shielded regions. In consequence, we adopt the more moderate value given in Table 1.

In Figure 1 we show the contributions to the gas cooling with standard abundances at a temperature of 10 K for a cloud with a velocity gradient of 1 km s^{-1} pc^{-1}. Several interesting general features may be noted here. The cooling from all species varies as $n^2(H_2)$ at low H_2 densities. This is what is expected for optically thin, subthermal conditions, which characterize the emission from CI and $C^{18}O$ and marginally from CS and ^{13}CO for $n(H_2) \leq 10^3$ cm^{-3}. The water emission is, however, highly optically thick for $n(H_2) \geq 10^3$ cm^{-3}, but the cooling, which is almost entirely from the 1_{10}–1_{01} transition at this low temperature, has the same quadratic dependence on the hydrogen density until the combination of collisions and trapping thermalize the transition at $n(H_2) \simeq 10^5$ cm^{-3}. Thus, the line emission and the cooling behave as "effectively optically thin" until this value of the H_2 density is reached (Linke et al. 1977; Snell et al. 2000a, 2000b). The cooling curves for $C^{18}O$ and CS are interesting in that they do not saturate even at the highest densities. This is because numerous transitions can effectively contribute to the cooling, and the transition that makes the largest contribution has a spontaneous decay rate that is sufficiently large that it is not thermalized even for the highest densities considered here. If there is only a single transition (as is the case for H_2O) or if the transitions that can contribute to the cooling are thermalized because of the combination of collisions and radiative trapping (as for ^{12}CO), the total cooling from that species does become constant as the density increases.

2.2. *Velocity Field and Cooling Calculation*

The velocity field in dark clouds is not well understood in detail, but here we assume that the large velocity gradient (LVG) approximation is valid for the radiative transfer calculations necessary to compute the molecular cooling when the optical depths are not small. The cloud is assumed to be spherical and the velocity to be purely radial, so the velocity gradient is the change in velocity per unit radius, dv/dr. While this represents a significant assumption about the cloud structure and the velocity field, we do not feel that it introduces a major uncertainty in the total cooling function, as discussed in Goldsmith & Langer (1978), Neufeld & Kaufman (1993), and Neufeld, Lepp, & Melnick (1995). A critical input to the LVG calculation is the molecular abundance per unit velocity gradient, $X/dv/dr$, which is equivalent to the column density per unit line width. Comparing the sizes and line widths for many clouds gives a characteristic value of 1 km s^{-1} pc^{-1}. In Figure 2 we give the cooling rate Λ per unit volume (in units of ergs cm^{-3} s^{-1}) as a function of the gas kinetic temperature (T_{gas}) and molecular hydrogen density $n(H_2)$ for the undepleted abundances given in Table 1. We see that for each value of the density, the cooling is reasonably well-represented by a power-law

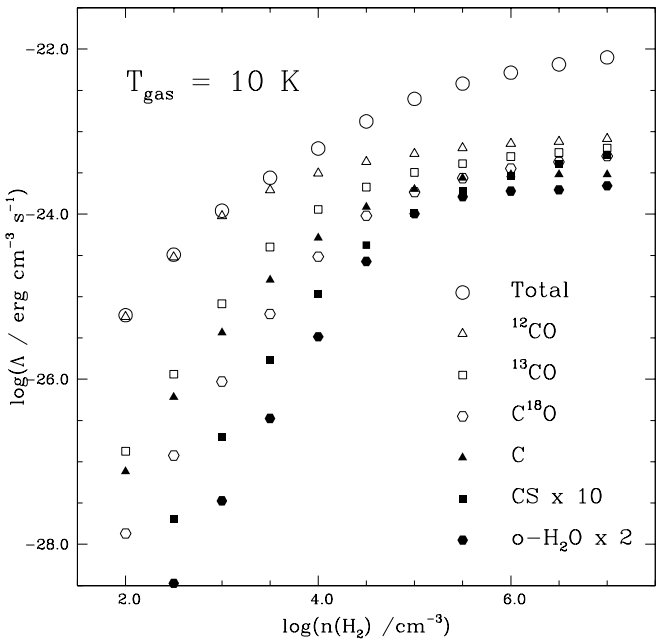

FIG. 1.—Contributions to the total gas cooling rate from various species as a function of H_2 density. The kinetic temperature is 10 K, the velocity gradient is 1 km s^{-1} pc^{-1}, and the fractional abundances are the undepleted standard values given in Table 1.

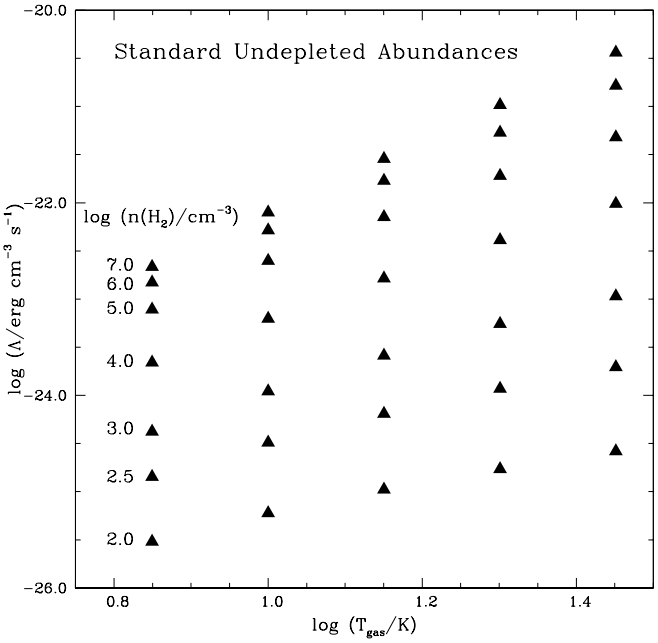

FIG. 2.—Cooling rate as a function of gas temperature and molecular hydrogen density. The undepleted abundances given in Table 1 have been used, as has a uniform spherical cloud with velocity gradient of 1 km s^{-1} pc^{-1}.

dependence on the temperature. If we parameterize the cooling function as

$$\Lambda_{\rm gas} = \alpha(T_{\rm gas}/10\ {\rm K})^{\beta}\ {\rm ergs\ cm^{-3}\ s^{-1}}\ , \qquad (1)$$

we obtain the results given in Table 2. The value of the exponent for the temperature dependence increases rapidly with increasing density. However, we note that for the conditions treated here, the cooling rate increases as a function of temperature approximately as rapidly as does that of a blackbody only for $n({\rm H_2}) \geq 10^6\ {\rm cm^{-3}}$.

If clouds are in virial equilibrium, they are not rigorously characterized by large-scale systematic motion, as required for the LVG approximation to be valid, but if we compute a velocity gradient from the ratio of cloud line width divided by cloud radius obtained from virial equilibrium for a uniform density sphere, we find

$$dv/dr \simeq 3.1\ {\rm km\ s^{-1}\ pc^{-1}}\sqrt{n({\rm H_2})/10^4\ {\rm cm^{-3}}}\ . \qquad (2)$$

This yields $dv/dr = 1\ {\rm km\ s^{-1}\ pc^{-1}}$ for a density of $10^3\ {\rm cm^{-3}}$, which is reasonably characteristic of dark clouds. The density of dark cloud cores is up to several orders of magnitude higher, and the velocity gradient in consequence will be larger if virial equilibrium is characteristic of these regions. To evaluate the effect of a velocity gradient that varies as a function of density, we have carried out cooling calculations for the undepleted abundances as used previously but with a density-dependent velocity gradient given by equation (2).

Specifically, we take $dv/dr = [n({\rm H_2})/10^3\ {\rm cm^{-3}}]^{0.5}\ {\rm km\ s^{-1}\ pc^{-1}}$ and show the results for a gas kinetic temperature of 10 K in Figure 3. The cooling rate is increased at densities below $10^3\ {\rm cm^{-3}}$ because dv/dr is smaller than $1\ {\rm km\ s^{-1}\ pc^{-1}}$, and the quantity $X/dv/dr$ is larger than for the constant velocity gradient case. This is equivalent to increasing the molecular abundances with a constant velocity gradient and hence increasing the cooling rate per unit volume. For low densities, the optical depths of cooling transitions are quite moderate so that for $n({\rm H_2}) = 10^2\ {\rm cm^{-3}}$, the cooling rate is increased by almost a factor of 3 for a decrease in the velocity gradient of $\sqrt{10}$. At high densities, the optical depths are so large that, although they are reduced relative to the constant velocity gradient case according to equation (2), the cooling is reduced by a considerably smaller factor. The reduction in $\Lambda_{\rm gas}$ is at most a factor of 3 in the $10^5\ {\rm cm^{-3}} \leq n({\rm H_2}) \leq 10^6\ {\rm cm^{-3}}$ range, in which the velocity gradient is a factor of 10–30 larger than at the reference density of $10^3\ {\rm cm^{-3}}$. The decrease in the cooling rate for a density of $10^7\ {\rm cm^{-3}}$ is even less. Although virial equilibrium would imply much larger velocity gradients than $1\ {\rm km\ s^{-1}\ pc^{-1}}$ for high densities, the effect on cloud cooling appears quite small. Given our lack of knowledge about the dynamical state of dense cloud cores, we adopt a velocity gradient of $1\ {\rm km\ s^{-1}\ pc^{-1}}$ for all densities in the following calculations, which has the further advantage of isolating the effect of varying molecular abundances.

TABLE 2

PARAMETERS[a] FOR GAS COOLING FUNCTION WITH STANDARD ABUNDANCES AND VELOCITY GRADIENT OF $1\ {\rm km\ s^{-1}\ pc^{-1}}$

$\log[n({\rm H_2}/{\rm cm^{-3}}]$	α	β
2.0	6.3×10^{-26}	1.4
2.5	3.2×10^{-25}	1.8
3.0	1.1×10^{-24}	2.4
4.0	5.6×10^{-24}	2.7
5.0	2.3×10^{-23}	3.0
6.0	4.9×10^{-23}	3.4
7.0	7.4×10^{-23}	3.8

[a] $\Lambda = \alpha(T_{\rm gas}/10\ {\rm K})^{\beta}$.

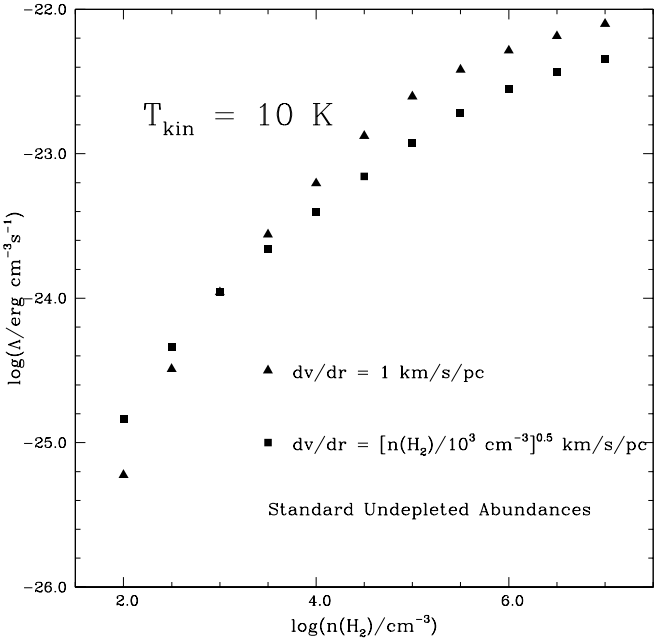

FIG. 3.—Comparison of cooling at the gas kinetic temperature of 10 K with undepleted abundances using two different laws for the velocity gradient, as discussed in the text.

The cooling functions derived here have essentially the same temperature dependence (values of β) as those presented by Goldsmith & Langer (1978). The present values of Λ are within a factor of 2 of those given by Goldsmith & Langer (1978) in the 10–20 K temperature range. The convenient generalized expression for Λ given by Nelson & Langer (1997) based on the calculations of Goldsmith & Langer (1978) give values of β (for fixed H_2 density) that are somewhat lower than given here in Tables 2 and 4, although the values of Λ are within a factor of 3. The larger fractional abundance for CS, taken here to represent "other" species, compared to the sum of the "other molecules" and "molecular ion" categories in Goldsmith & Langer (1978), evidently offsets the order-of-magnitude lower fractional abundance of CI adopted in the present work. The present calculations confirm that the temperature dependence of Λ is weaker at higher values of $T_{\rm gas}$.

2.3. *Depletion and the Gas Cooling Rate*

The uncertainties in depletion and desorption processes and rates (mentioned briefly in § 1) suggest that we should treat the molecular abundances in a parametric fashion. The observational results on depletion of different species are relatively limited and are certainly compromised by the blending of emission from different regions along the line of sight. There also have not yet been systematic studies of the depletion of a wide range of molecular species in a set of sources, so we are limited to dealing with fragmentary data from a selection of clouds. The typical values reported for the rare isotopes of carbon monoxide are factors of 3–20

(see, e.g., Gibb & Little 1998; Willacy et al. 1998b; Caselli et al. 1999; Kramer et al. 1999). Dark clouds detected by the *Midcourse Space Experiment* exhibit formaldehyde depletion factors (DFs) $\simeq 50$ (Carey et al. 1998), while several nearby dark clouds studied in detail exhibit significant depletions in CCS and CS (Ohashi et al. 1999; Kuiper et al. 1996).

Rather than try to specifically model these results, we adopt a more schematic approach and parameterize the depletion via a single DF defined as the standard abundance by the actual abundance. We give these in logarithmic form in Table 3. The values of DF represent the depletion of carbon monoxide isotopes and CS, which collectively represent the bulk of molecular coolant species expected to deplete. We consider the abundances of atomic carbon and oxygen to remain constant and allow the abundance of gas-phase H_2O to decrease only modestly since it is plausible that this species is significantly depleted onto dust grain surfaces even for the run with standard abundances. DF0.3 is a run in which the abundances of all molecular species are *increased* by a factor of $\sqrt{10}$ relative to standard values.

The depletion of the major molecular coolants results in a significant reduction of the cooling rate at low densities, at which ^{12}CO and ^{13}CO are the two most important individual coolants, particularly at low temperatures (Fig. 1). At 10 K, the total cooling for DF100 is reduced by a factor of 40 at $n(H_2) = 10^2$ cm^{-3}, and the contribution from C is about 80% of that of ^{12}CO. However the total cooling rate at a density of 10^7 cm^{-3} is reduced by only a factor ≤ 2; that of the ^{12}CO is not significantly different because of its very high optical depth, and only the contributions of the species whose cooling is effectively optically thin are reduced appreciably.

The gas-phase cooling rates for different DFs at densities of 10^4 and 10^5 cm^{-3} are shown in Figure 4, and the values

TABLE 3

LOGARITHMIC ABUNDANCES OF VARIOUS SPECIES COMPARED TO STANDARD VALUES FOR DIFFERENT DEPLETION RUNS

Species	DF0.3	DF1	DF3	DF10	DF30	DF100
^{12}CO	0.5	0.0	−0.5	−1.0	−1.5	−2.0
^{13}CO	0.5	0.0	−0.5	−1.0	−1.5	−2.0
$C^{18}O$	0.5	0.0	−0.5	−1.0	−1.5	−2.0
C	0.0	0.0	0.0	0.0	0.0	0.0
o-H_2O	0.5	0.0	−0.5	−1.0	−1.0	−1.0
$^{12}C^{32}S$	0.5	0.0	−0.5	−1.0	−1.5	−2.0
O	0.0	0.0	0.0	0.0	−0.5	−0.5

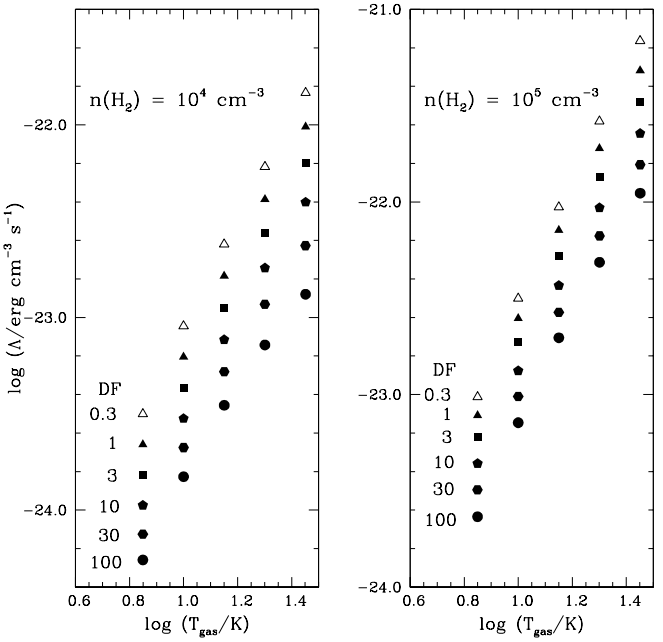

FIG. 4.—Total gas cooling rates as a function of temperature for runs with different DFs, as defined in Table 3. The left-hand panel is for an H_2 density of 10^4 cm^{-3}, and the right hand panel is for an H_2 density a factor of 10 greater.

of the parameters for the cooling function as defined in equation (1) are given in Table 4. The most significant result is the weak dependence of the cooling on the DFs. For $n(H_2) = 10^4$ cm^{-3}, going from DF1 to DF100 reduces the cooling by only a factor of 4 for $T_{gas} = 7$ K and by a factor of 8 for $T_{gas} = 31.6$ K. This insensitivity is a direct result of the cooling being dominated by optically thick emission. The slightly greater dependence on DF at the high temperature is a consequence of the reduction in the optical depths produced by the increase in the number of energy levels with a significant population. The situation is even more extreme for the density of 10^5 cm^{-3} because of the larger column densities of molecules; in this situation the reduction in cooling between DF1 and DF100 varies only between a factor of 4 and 5 over the range of temperatures considered here.

The slope of the cooling curve as defined by β (eq. [1]) does drop somewhat as the depletion increases, but it is also the case that a power law is a less accurate representation for larger depletions.

TABLE 4

PARAMETERS[a] FOR GAS COOLING FUNCTION FOR DIFFERENT DEPLETION RUNS

	$n(H_2) = 10^3$ cm^{-3}		$n(H_2) = 10^4$ cm^{-3}		$n(H_2) = 10^5$ cm^{-3}		$n(H_2) = 10^6$ cm^{-3}	
DEPLETION RUN	log α	β	log α	β	log α	β	log α	β
DF1	−24.0	2.4	−23.3	2.7	−22.6	3.0	−22.3	3.4
DF3	−24.2	2.1	−23.4	2.7	−22.8	2.9	−22.4	3.3
DF10	−24.5	1.9	−23.5	2.6	−22.9	2.8	−22.4	3.2
DF30	−24.8	1.8	−23.7	2.5	−23.0	2.8	−22.5	3.2
DF100	−25.1	1.8	−23.8	2.2	−23.2	2.8	−22.6	3.1

NOTE.—The units of α are ergs cm^{-3} s^{-1}.

[a] $\Lambda = \alpha(T_{gas}/10\ \mathrm{K})^{\beta}$; velocity gradient = 1 km s^{-1} pc^{-1}.

3. OTHER HEATING AND COOLING PROCESSES

To calculate the thermal balance within dark cloud cores, we need to consider processes affecting the gas and the dust in addition to the radiative gas cooling discussed above. In this section we briefly discuss the different heating and cooling processes and rates for the gas and dust separately as well as for the gas-dust coupling.

Since we are interested in well-shielded regions, we can reasonably ignore processes such as the photoelectric heating of the gas. We consider cosmic rays to be the only process that heats the gas directly. The heating rate can be considered to be the product of the cosmic-ray ionization rate ζ_0 multiplied by the energy input per ionization ΔQ. Goldsmith & Langer (1978) adopt a value of $\zeta_0 = 2 \times 10^{-17}$ s^{-1}, while van Dishoeck & Black (1986) suggest a value of 7×10^{-17} s^{-1}. The value of ΔQ is approximately 20 eV. We adopt here for the cosmic-ray heating rate per unit volume

$$\Gamma_{\rm gas,\ cr} = 10^{-27}[n({\rm H}_2)/{\rm cm}^{-3}]\ {\rm ergs\ cm}^{-3}\ {\rm s}^{-1}\ , \qquad (3)$$

which is intermediate between the values obtained using the different ionization rates mentioned above.

Even in an "average" environment, an interstellar cloud will have radiation from the diffuse UV-visible-IR interstellar radiation field (ISRF) incident on its surface. This "unattenuated" radiation field will heat dust grains to temperatures greater than those observed for dark cloud cores. This can be seen, e.g., in Figure 3 of Mathis, Mezger, & Panagia (1983) and from the dust temperatures of 14–17 K derived by Lehtinen et al. (1998) in the Thumbprint Nebula, a cloud with visual extinction $A_v \simeq 4$ mag.

To model the low temperatures ($\lesssim$10 K) characteristic of dark cloud cores in which depletion is likely to be significant, we need to consider the attenuation of the ISRF due to the dust grains. Rather than utilize a specific self-consistent radiative transfer model, we can make a reasonable approximation by considering that there is a component of the diffuse ISRF, scaled by a factor χ, that heats the dust grains located in the region of interest. This ignores the reradiation by grains from elsewhere in the cloud, but for a dark cloud with only the ISRF to start with, the grain temperatures (discussed further below) are so low that their reradiation occurs primarily at far-infrared wavelengths. The grain absorption cross sections at these long wavelengths are so small compared to those at near-infrared and visible wavelengths that the dust heating will be dominated by the attenuated radiation rather than the cloud's internal radiation unless χ is extremely small.

We take F_0, the unattenuated flux from the diffuse ISRF, equal to 5.3×10^{-3} ergs cm^{-2} s^{-1}. This is consistent with the integrated intensity between 0.09 and 8 μm at a Galactocentric distance of 10 kpc given by Mathis et al. (1983) and with the "stellar" component of the radiation density given by Allen (1976, p. 268). Achieving dust temperatures in the range of interest (6–10 K) requires values of χ of 10^{-4} to 10^{-5}, corresponding nominally to visual extinctions to the surface in the 10–12 mag range. These values are consistent with the range expected for dark cloud cores, e.g., $A_v \geq$ 10 mag in high-extinction cores studied by Kramer et al. 1999 and A_v inferred to be 50 mag in the study of the L1498 core by Willacy et al. (1998b). The dust temperature does not continue to drop for extinctions much greater than this because of the heating provided by the reemision from dust grains themselves, as seen, e.g., in the calculations of Werner & Salpeter (1969) and Mathis et al. (1983). The present parameterization of the radiation field can be considered to characterize the total dust heating in moderately well-shielded regions of the cloud.[3]

The dust heating rate per cubic centimeter produced by the external radiation field is given by

$$\Gamma_{\rm dust,\ ext} = n_d\, \sigma_d(\nu_h) F_0\, \chi\ , \qquad (4)$$

where n_d is the density of dust grains and σ_d is the absorption cross section of a grain at the frequencies relevant for heating. The dust quantities are related to the hydrogen density through the expression

$$n_d\, \sigma_d(\nu) = \frac{3Q(\nu)}{4a\rho_g}\, \frac{n({\rm H}_2) m({\rm H}_2)}{G/D}\ , \qquad (5)$$

where we have assumed a single type of dust grain having radius a and density ρ_g. The quantity $Q(\nu)$ is the ratio of absorption (or emission) cross section to geometrical cross section at frequency ν, G/D is the gas-to-dust ratio by mass, and $m({\rm H}_2)$ is the mass of a hydrogen molecule.

We adopt $a = 1.7 \times 10^{-7}$ cm, $\rho_g = 2$ g cm^{-3}, and $G/D = 100$. For the frequencies at which heating from external ISRFs is significant, we can take $Q(\nu)$ equal to unity since this process occurs at wavelengths $\simeq a$. This gives us

$$n_d\, \sigma_d(\nu_h) = 7.4 \times 10^{-22}[n({\rm H}_2)/{\rm cm}^{-3}]\ {\rm cm}^{-1}\ , \qquad (6)$$

and the dust heating rate per unit volume from the external radiation field becomes

$$\Gamma_{\rm dust,\ ext} = 3.9 \times 10^{-24}[n({\rm H}_2)/{\rm cm}^{-3}]\chi\ {\rm ergs\ cm}^{-3}\ {\rm s}^{-1}\ . \qquad (7)$$

The gas cooling by spectral line radiation has been discussed above, but the dust cooling must also be considered. At the temperatures of relevance here, the dust cooling takes place at wavelengths at which the dust is optically thin because of the small values of $Q(\nu)$ for $\lambda \gg a$. The dust absorption coefficient $\kappa(\nu)$ is just given by equation (5) with the appropriate value of Q.

We normalize the dust absorption coefficient to the average value for three GMCs studied by Goldsmith et al. (1997). At their reference wavelength of 790 μm, $\nu_0 = 3.8 \times 10^{11}$ Hz, and the derived dust absorption efficiency is $Q(\nu_0) = 4.5 \times 10^{-5}$. This is relatively close to the value of 3.3×10^{-5} calculated by Draine (1985) for silicate grains and also reasonably consistent with $Q(\nu_0) = 9 \times 10^{-5}$ found for core mantle grains by Preibisch et al. (1993). From the observationally determined value of $Q(\nu_0)$, we find that the dust absorption coefficient at the reference frequency is

$$\kappa(\nu_0) = 3.3 \times 10^{-26}[n({\rm H}_2)/{\rm cm}^{-3}]\ {\rm cm}^{-1}\ , \qquad (8)$$

We assume that the dust optical depth varies as ν^2, which is a reasonable description of observations of dust in better-studied GMCs (see discussion in Goldsmith et al. 1997) and

[3] This behavior has been confirmed by using the computer code DUSTY Ivezić, Nenkova, & Elitzur 1999. The code was configured to model a uniform density spherical cloud with the standard ISRF as an external heating source, treating the radiative transfer in a self-consistent manner. The grains were a mixture of silicate and graphite grains, as defined by Draine & Lee (1984). We find that a visual extinction of approximately 8 mag measured from the cloud surface is required to have the average grain temperature drop to $\simeq$10 K.

which plausibly applies to dark cloud cores as well. The dust absorption coefficient throughout the submillimeter is thus given by

$$\kappa(\nu) = \kappa(\nu_0)[\nu/3.8 \times 10^{11}\ \mathrm{Hz}]^2\ \mathrm{cm}^{-1}\ . \quad (9)$$

This gives the dust optical depth in terms of $N(H_2)$, the column density of molecular hydrogen through the cloud,

$$\tau_{\mathrm{dust}}(\nu) = 3.3 \times 10^{-26}(\nu/3.8 \times 10^{11}\ \mathrm{Hz})^2[N(H_2)/\mathrm{cm}^{-2}]\ . \quad (10)$$

For a visual extinction of 30 mag, $N(H_2) \simeq 3 \times 10^{22}$ cm^{-2} and $\tau(\nu) = 10^{-3}\ (\nu/3.8 \times 10^{11}\ \mathrm{Hz})^2$. The optical depth reaches a value of 0.1 only at a wavelength of 80 μm, for which $h\nu/k = 180$ K. For cloud temperatures $\simeq 10$ K, the radiation at infrared and shorter wavelengths is seen to be negligible, and the optically thin assumption is justified.

The dust emission is determined by the dust temperature T_d and the dust emissivity (given in eq. [9]) through the equation

$$\Lambda_{\mathrm{dust}} = c \int U_\nu(T_d)\kappa(\nu)d\nu\ , \quad (11)$$

where $U_\nu(T)$ is the Planck energy density at frequency ν produced by a blackbody at temperature T. Although the frequency dependence of the dust emissivity given by equation (9) does not likely extend to wavelengths shorter than $\simeq 50$ μm, for the low temperatures considered here, the error in extending the integral to cover all frequencies is negligible. The result for the dust cooling rate is

$$\Lambda_{\mathrm{dust}} = 2.9 \times 10^{16} T_d^6\, \kappa(\nu_0)/\nu_0^2\ , \quad (12)$$

which for the values normalizing the dust emission adopted (eq. [8]) gives us a dust cooling rate per unit volume

$$\Lambda_{\mathrm{dust}} = 6.8 \times 10^{-33}(T_d/\mathrm{K})^6[n(H_2)/\mathrm{cm}^{-3}]\ \mathrm{ergs\ cm}^{-3}\ \mathrm{s}^{-1}\ . \quad (13)$$

An important contributor to the cloud thermal balance is the energy transfer between dust and gas due to collisions. This is usually described in terms of the difference in energy of an H_2 molecule before and after each collision with a dust grain. The gas-dust energy transfer rate per unit volume can then be written as (Burke & Hollenbach 1983)

$$\Lambda_{\mathrm{gd}} = n(H_2)\langle\sigma_d v_{H_2}\rangle n_d\, \alpha(2kT_{\mathrm{gas}} - 2kT_{\mathrm{dust}})\ , \quad (14)$$

where σ_d and n_d are the cross section and density of a dust grain, respectively. We take $\alpha = 0.3$ (Burke & Hollenbach 1983) for H_2 particles, and putting in canonical values for the dust to gas ratio and the dust grain cross section, we obtain

$$\Lambda_{\mathrm{gd}} = 2 \times 10^{-33}[n(H_2)/\mathrm{cm}^{-3}]^2(\Delta T/\mathrm{K}) \times (T_{\mathrm{gas}}/10\ \mathrm{K})^{0.5}\ \mathrm{ergs\ cm}^{-3}\ \mathrm{s}^{-1}\ , \quad (15)$$

where we have defined

$$\Delta T = T_{\mathrm{gas}} - T_{\mathrm{dust}}\ \mathrm{K}\ . \quad (16)$$

When the gas temperature is greater than the dust temperature, the gas heats the dust, and with this definition ΔT and Λ_{gd} are positive.

4. THERMAL BALANCE CALCULATIONS

To determine the thermal balance of gas and the dust, coupled together by the gas-dust collisions, we solve simultaneously the equations

$$\Gamma_{\mathrm{gas,\ cr}} - \Lambda_{\mathrm{gas}} - \Lambda_{\mathrm{gd}} = 0 \quad (17)$$

and

$$\Gamma_{\mathrm{dust,\ ext}} - \Lambda_{\mathrm{dust}} + \Lambda_{\mathrm{gd}} = 0\ . \quad (18)$$

Results for different hydrogen densities, depletions, and flux-scaling factors are presented in Table 5. In the table, the first three columns identify the depletion run (Table 3), the molecular hydrogen density $n(H_2)$, and the flux-scaling factor χ, while the columns $T_{\mathrm{gas,\ 0}}$ and $T_{\mathrm{dust,\ 0}}$ give the gas and dust temperatures in the absence of gas-dust coupling, respectively.

The general effect of the coupling between the gas and the dust is illustrated in Figure 5. Without the coupling between the gas and the dust, the gas temperature rises somewhat for $n(H_2) < 10^{2.5}$ cm^{-3} because of the relatively inefficient cooling at low densities compared to the cosmic-ray heating, having a constant rate per H_2 molecule. At high densities [$n(H_2) > 10^{3.5}$ cm^{-3}], the gas temperature also rises because the cooling efficiency is reduced due to the thermalization and high opacity in key cooling lines. At intermediate densities, the gas temperature reaches a minimum value of approximately 10 K. The situation at low and intermediate densities is not significantly affected by the inclusion of gas-dust coupling since its effect varies as the square of the density (eq. [15]). However, for densities above 10^4 cm^{-3}, the effect is quite dramatic, with the gas temperature being reduced to below 10 K at the highest densities, while the dust temperature is increased by only 1–2 K. This is a direct result of the extremely strong temperature dependence of the dust cooling (eq. [13]). With sufficiently rapid energy transfer between the dust and gas,

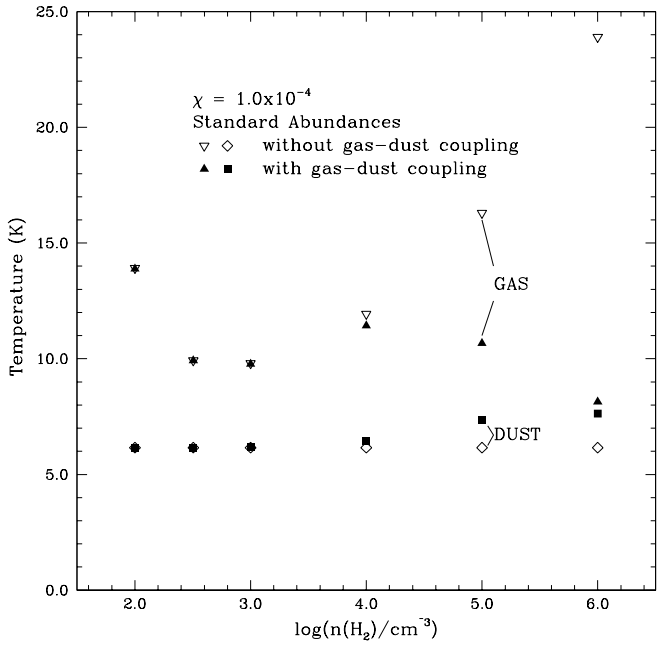

FIG. 5.—Effect of gas-dust coupling on gas and dust temperatures in a well-shielded region with $\chi = 1.0 \times 10^{-4}$. The undepleted standard values of the molecular abundances (Table 1) are used. The open symbols describe the situation without gas-dust coupling, while the filled symbols show the effect of including the coupling between the two species. The coupling significantly reduces the gas temperature at higher densities [$n(H_2) > 10^4$ cm^{-3}] while only slightly raising the dust temperature.

TABLE 5

DUST AND GAS TEMPERATURES

Depletion Run	T_{gas} (K)	T_{dust} (K)	$T_{gas,0}$ [a] (K)	$T_{dust,0}$ [b] (K)
$\log[n(H_2)/cm^{-3}] = 3.0; \log\chi = -4.0$				
DF1	9.77	6.18	9.80	6.16
DF3	12.6	6.20	12.7	6.16
DF10	17.9	6.24	18.2	6.16
DF30	26.6	6.34	27.7	6.16
DF100.....	37.4	6.46	40.2	6.16
$\log[n(H_2)/cm^{-3}] = 4.0; \log\chi = -4.0$				
DF1	11.4	6.53	11.9	6.16
DF3	12.9	6.52	13.8	6.16
DF10	14.8	6.63	16.2	6.16
DF30	16.7	6.74	18.9	6.16
DF100.....	19.2	6.89	23.5	6.16
$\log[n(H_2)/cm^{-3}] = 5.0; \log\chi = -4.0$				
DF1	10.7	7.37	16.3	6.16
DF3	11.0	7.43	18.4	6.16
DF10	11.2	7.49	20.7	6.16
DF30	11.4	7.54	23.8	6.16
DF100.....	11.6	7.56	26.4	6.16
$\log[n(H_2)/cm^{-3}] = 6.0; \log\chi = -4.0$				
DF1	8.14	7.63	23.9	6.16
DF3	8.15	7.64	26.4	6.16
DF10	8.16	7.64	28.2	6.16
DF30	8.18	7.64	30.7	6.16
DF100.....	8.18	7.64	32.8	6.16
$\log[n(H_2)/cm^{-3}] = 3.0; \log\chi = -3.0$				
DF1	9.78	9.04	9.80	9.04
DF3	12.6	9.04	12.7	9.04
DF10	18.0	9.05	18.2	9.04
DF30	26.8	9.06	27.7	9.04
DF100.....	37.6	9.08	40.2	9.04
$\log[n(H_2)/cm^{-3}] = 4.0; \log\chi = -3.0$				
DF1	11.7	9.06	11.9	9.04
DF3	13.2	9.08	13.8	9.04
DF10	15.2	9.10	16.2	9.04
DF30	17.1	9.12	18.9	9.04
DF100.....	19.8	9.16	23.5	9.04
$\log[n(H_2)/cm^{-3}] = 5.0; \log\chi = -3.0$				
DF1	11.9	9.27	16.3	9.04
DF3	12.8	9.30	18.4	9.04
DF10	12.6	9.32	20.7	9.04
DF30	12.8	9.35	23.8	9.04
DF100.....	13.0	9.36	26.4	9.04
$\log[n(H_2)/cm^{-3}] = 6.0; \log\chi = -3.0$				
DF1	9.84	9.39	23.9	9.04
DF3	9.86	9.39	26.4	9.04
DF10	9.86	9.39	28.2	9.04
DF30	9.86	9.39	30.7	9.04
DF100.....	9.86	9.40	32.8	9.04

[a] Gas temperature without gas-dust coupling.
[b] Dust temperature without gas-dust coupling.

the dust cooling is sufficient to maintain a very low gas temperature, with the dust and gas temperatures becoming essentially equal for $n(H_2) \geq 10^6$ cm^{-3}.

The effect of the molecular depletion, with the gas-dust coupling included, is summarized in Figure 6. We here have adopted a flux-scaling factor $\chi = 10^{-4}$ in order to get a dust temperature in the range observed for dark clouds without star formation. We see that at low to moderate densities, the depletion has the effect of raising the gas temperature appreciably. This is a combination of the gas-dust coupling being ineffective for hydrogen densities below 10^4 cm^{-3} with the moderate exponent of the temperature dependence of the gas cooling (β; eq. [1]; Table 4). The result is that the moderate reduction in the cooling rate produced by the depletion of major coolant species does result in a significant increase in the gas temperature from 10 (DF1) to almost 40 K (DF100) at a hydrogen density of 10^3 cm^{-3}. At even lower densities, the effect would be yet more dramatic, but it is likely that such regions would have sufficiently low extinction that other heating processes would come into play.

At higher densities, the increase in the gas temperature is much reduced by the coupling to the dust. At a density of 10^5 cm^{-3}, the increase in the gas temperature is no more than 1 K even for depletions of the main coolant species by a factor of 100. For $n(H_2) = 10^6$ cm^{-3}, the gas and dust are both at a temperatures close to 9 K for all of the depletion runs considered here. It is the case that for even greater depletions, the gas cooling will be reduced to the point that the gas temperature will rise despite the gas-dust coupling. Given that there will almost certainly be some species that

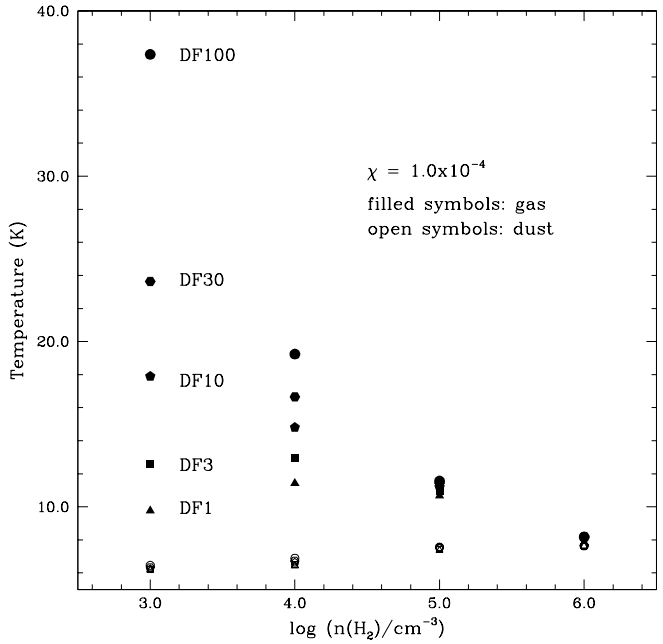

FIG. 6.—Solutions for the dust and gas temperatures for different molecular hydrogen densities and depletion runs for flux-scaling parameter $\chi = 1.0 \times 10^{-4}$. For each set of conditions, the filled symbol gives the gas temperature, and the open symbol gives the dust temperature; the latter are so nearly equal for each group of DFs that they are not individually labeled. It is evident that at low densities, the gas temperature rises significantly when the gas cooling efficiency is reduced because of depletion, but at densities greater than 10^4 cm^{-3}, the gas-dust coupling holds the gas temperature to a relatively low, essentially fixed value, while the dust temperature increases only slightly, by less than 2 K.

are bound only weakly to grains and that remain to a significant degree in the gas phase, it is challenging to model much larger DFs with any confidence. However, the trend of rising gas temperature with increasing DF seen in Table 5 continues.[4] This suggests that if core conditions and lifetimes do permit DFs in excess of 100, the gas temperature will rise significantly even for reasonably high densities $n(H_2) \geq 10^5$ cm^{-3}.

5. DISCUSSION

5.1. *Depletion and Thermal Balance*

This study has reinforced the importance of considering the coupling between gas and dust when analyzing the thermal balance within well-shielded regions of dark clouds. In regions with densities exceeding $10^{4.5}$ cm^{-3}, the dust and gas temperatures will be relatively closely coupled. At a density of 10^6 cm^{-3}, the gas temperature is below 10 K when gas-dust coupling is included, as compared to 25 K if it is neglected. To analyze fully the impact on the gas temperature and the possible thermal support of dense regions would require a more accurate treatment of the infrared radiative transfer, but it is clear that simple statements based exclusively on gas heating and cooling processes (see, e.g., Clarke & Pringle 1997) will not apply when densities begin to increase significantly.

The effect of depletion of coolant species on the gas cooling rate is found to be moderated by the large optical depths in the important cooling lines. At a temperature of 10 K, a factor of $\simeq 100$ reduction in abundances produces only a factor $\simeq 4$ reduction in the cooling per unit volume. The reduction in Λ_{gas} is a factor of $\simeq 10$ for the same DF at higher temperatures, where the distribution of molecules over more levels results in lower opacities.

The effect of even this reduction in gas-phase cooling is significant at low densities, however, because of the relatively weak temperature dependence of the cooling rate under these conditions. At a molecular hydrogen density of 10^3 cm^{-3}, a factor of 10 depletion of molecular coolant species increases the gas temperature from 10 to 18 K. The low gas-dust coupling suggests that the dust temperatures will not be significantly affected by the depletion process. In consequence, if there is sufficient time for depletion to become significant in regions of low to moderate density (where depletion timescales are necessarily relatively long), we might see warmer gas coexisting with cool dust.

The present model provides an interesting constraint on the interpretation of the small dark clouds studied by Lemme et al. (1996). The ammonia and $C^{18}O$ observations of these regions indicate relatively uniform gas temperatures close to 10 K, with hydrogen densities concentrated in the 4×10^3–2×10^4 cm^{-3} range. These values are consistent with our modeling only if there is essentially no depletion. Conversion of the observed $C^{18}O$ line intensity to H_2 column density carried out with this assumption yields reasonable results in terms of virial equilibrium of these globules. There may be some depletion in the higher density globules included in this study but they nevertheless have maintained relatively low gas temperatures. This would suggest that these globules are fairly young, but it is also possible that the dust temperatures in these regions are enhanced since their total visual extinctions ≤ 6 mag.

At higher densities, the increased gas-dust coupling overwhelms the reduced gas-phase cooling, and we see a decrease in the gas temperature, in contrast to the expected increase. The gas temperature is held at approximately 9 K for DFs up to 100 at a density of 10^6 cm^{-3}, while the dust temperature has increased by less than 0.5 K as a consequence of its cooling the gas. The depletion process can thus proceed to a marked extent without there being any significant change in either the dust or the gas temperature that would offer any feedback in terms of increasing the desorption rate due to a dust temperature increase or that would be observable in terms of an increase in the gas temperature as a consequence of the reduced gas cooling rate. This modeling is consistent with the observed factors of 10–100 depletions from the gas phase in well-shielded regions, provided only that the density in these regions is larger than 10^4 cm^{-3}, which agrees with data in cases where the density can be independently determined. Thus, depletion is likely to be important on timescales $\geq 10^5$ yr and can not only change the emission from cores but can also have specific effects on diagnostics such as modifying the signature of infall motions in very dense regions, as pointed out by Wilner et al. (2000).

That molecular depletion can proceed without affecting the thermal balance of dense regions suggests that this process may have a significant impact on the degree of ionization of the gas phase as well. Among the important coolant species are some of the most abundant molecular ions (HCO^+, N_2H^+, ...), and if these deplete appreciably (assuming that electrons deplete in proportion so that the net grain charge does not vary much), the ionization fraction of the gas will certainly be reduced. The charged grains can still couple to the magnetic field (Elmegreen 1979), but the depletion of charged species can certainly have an impact on the coupling of the gas phase to the magnetic field, with obvious consequences for the dynamical evolution of dense cores.

The fact that molecular depletion raises the gas temperature more in regions where the density is lower provides an interesting mechanism for pressurizing dense cloud cores. We see from Figure 6 that if the depletion increases as a function of time, the gas temperature in lower density regions will rise relative to that in regions of higher density. Thus, the external thermal pressure on a denser condensation will increase. While this effect may be modest, perhaps only a factor of 3, it will help confine the denser regions and may accelerate the collapse of the condensations. The signature of this effect would be a region in which the gas temperature is enhanced relative to that of the dust; it would presumably surround a denser, cold core, and would have to be within a region having visual extinction ≥ 5 mag. This would not be easy to detect observationally but could nevertheless be a significant ingredient in the structure of dark clouds and the relationship of dense cores to the star formation found within them.

5.2. *Uncertainties in Modeling*

The present modeling effort has made several assumptions that do limit our confidence about detailed conclu-

[4] As a relatively extreme example, we deplete molecular coolant species by a factor of 1000 and atomic species by a factor of 100, which reduces the cooling rate by a factor of $\simeq 4$ below that of DF100. The cooling is still dominated by ^{12}CO, but its emission is becoming effectively thin even for a density equal to 10^5 cm^{-3}. The cooling from hydrides including HD is quite unimportant at the low temperatures considered here despite the large molecular depletion. With $\chi = 10^{-4}$, the gas temperature is 12 K and the dust temperature is 7.7 K for $n(H_2) = 10^5$ cm^{-3}.

sions. The calculation of the molecular cooling itself is dependent on the radiative transfer in the optically thick cooling lines, which in general are important contributors to the total gas cooling. The use of the LVG model introduces some uncertainty here, as does the choice of the velocity gradient. However, we feel that these do not significantly alter the total cooling and the thermal balance except in extreme situations. The model for depletion is highly simplified since it ignores the selective depletion of different species (e.g., polar vs. nonpolar molecules), the variety of effects that may be introduced by the grain surface (due to, e.g., coverage by ices), and the detailed operation of different desorption mechanisms.

The choice of the DF should thus be taken as representative of an overall degree of depletion and not as a detailed representation of the molecular abundances at a particular stage of a cloud's evolution. The general picture we present is consistent with currently available observations and is suggestive of moderate depletion of some high dipole moment species (such as CS and H_2CO) as well as of the important tracer and coolant carbon monoxide and its isotopic variants. The plausible degree of depletion of each species that is likely to obtain in a given situation at a given time is uncertain and should be better determined by detailed modeling.

6. SUMMARY

We have combined a parameterized description of the depletion of coolant species with a calculation of the thermal balance of the dense, well-shielded regions of molecular clouds. We have used the LVG model for radiative transfer and considered clouds with molecular hydrogen densities between 10^2 and 10^7 cm^{-3}. Heating processes are cosmic-ray heating of the gas and dust heating by attenuated visible/infrared radiation characterized by the flux-scaling factor χ relative to standard ISRF. The dust cools via emission of optically thin far-infrared radiation, and the dust and gas are coupled through collisions.

The main conclusions are the following:

1. The low gas-phase H_2O abundance and O_2 upper limits in GMCs determined by *SWAS*, taken, as seems plausible, to apply to dark clouds as well, indicate that carbon monoxide and its isotopic variants, together with the ensemble of high dipole moment species (CS, HCN, N_2H^+, ...), are the dominant gas-phase coolants for low-temperature regions.

2. The molecular cooling is diminished by depletion, but because of the significant contribution of optically thick lines, the reduction in cooling efficiency is relatively modest—a factor of approximately 4 for a factor of 100 reduction in the abundance of major molecular coolants.

3. The depletion can significantly increase the gas temperature at low to moderate densities, $n(H_2) \leq 10^4$ cm^{-3}, with T_{gas} increasing from 10 to 40 K at $n(H_2) = 10^3$ cm^{-3} for a factor of 100 depletion in the major molecular coolant species.

4. The coupling between the dust and the gas plays a critical role in the thermal balance at higher densities. The dust cooling is so sensitive to its temperature ($\Lambda \simeq T_{dust}^6$), that once the density is sufficient to couple the gas and the dust together, the gas temperature is held at a relatively low value without appreciably increasing the dust temperature for DFs up to 100.

5. For densities $\geq 10^{4.5}$ cm^{-3}, there can be significant molecular depletion without an accompanying increase in the gas temperature or without there being significant self-regulation in terms of increased dust temperature limiting the molecular depletion. The depletion-induced enhancement of the thermal gas pressure in the lower density region surrounding a dense core may assist in the confinement of the central region or encourage its collapse.

I acknowledge with pleasure numerous helpful discussions with Ted Bergin and Malcolm Walmsley about depletion and cloud thermal balance. I thank A. Hjalmarson, D. Hollenbach, and W. Langer for suggestions that improved the paper. I also appreciate the careful reading and suggestions by John Black, the reviewer. I am very grateful to M. Elitzur and M. Nenkova for working to enhance their computer code DUSTY to deal with modeling dark clouds with external radiation fields. Part of this work was carried out while the author was enjoying the hospitality of the Max Planck Institut für Radioastronomie, Bonn, the École Normale Supérieure, Paris, and the Osservatorio Astrofisico di Arcetri, Florence. I thank Karl Menten, Edith Falgarone, and Gianni Tofani for their support during my stay at their respective institutions. The National Astronomy and Ionosphere Center is supported by a Cooperative Agreement with the National Science Foundation. This research was also supported in part by NASA through the *SWAS* project.

REFERENCES

Aikawa, Y., Umebayashi, T., Nakano, T., & Miyama, S. 1997, ApJ, 486, L51
Allen, C. W. 1976, Astrophysical Quantities (London: Athlone)
Ashby, M. L. N., et al. 2000, ApJ, 539, L115
Bergin, E. A., Langer, W. D., & Goldsmith, P. F. 1995, ApJ, 441, 222
Brown, P. D., Charnley, S. B., & Millar, T. J. 1988, MNRAS, 231, 409
Burke, J. R., & Hollenbach, D. J. 1983, ApJ, 265, 223
Carey, S. J., Clark, F. O., Egan, M. P., Price, S. D., Shipman, R. F., & Kuchar, T. A. 1998, ApJ, 508, 721
Caselli, P., Walmsley, C. M., Tafalla, M., Dore, L., & Myers, P. C. 1999, ApJ, 523, L165
Caux, E., et al. 1999, A&A, 347, L1
Clarke, C. J., & Pringle, J. E. 1997, MNRAS, 288, 674
Draine, B. T. 1985, ApJS, 57, 587
Draine, B. T., & Lee, H. M. 1984, ApJ, 285, 89
Dzegilenko, F., & Herbst, E. 1995, ApJ, 443, L81
Elmegreen, B. G. 1979, ApJ, 232, 729
Flower, D. R., & Launay, J. M. 1985, MNRAS, 214, 271
Frerking, M. A., Keene, J., Blake, G. A., & Phillips, T. G. 1989, ApJ, 344, 311
Frerking, M. A., Langer, W. D., & Wilson, R. W. 1982, ApJ, 262, 590
Gibb, A. G., & Little, L. T. 1998, MNRAS, 295, 299
Gibb, E. L., et al. 2000, ApJ, 536, 347
Goldsmith, P. F., Bergin, E. A., & Lis, D. C. 1997, ApJ, 491, 615
Goldsmith, P. F., & Langer, W. D. 1978, ApJ, 222, 881
Goldsmith, P. F., et al. 2000, ApJ, 539, L123
Green, S., & Chapman, S. 1978, ApJS, 37, 169
Hasegawa, T. I., & Herbst, E. 1993, MNRAS, 261, 83
Hasegawa, T. I., Herbst, E., & Leung, C. M. 1992, ApJS, 82, 167
Hoban, S., Reuter, D. C., Mumma, M. J., & Storrs, A. 1991, ApJ, 370, 228
Ivezić, Z., Nenkova, M., & Elitzur, M. 1999, User Manual for DUSTY, Univ. Kentucky Internal Rep. (astro-ph/9910475)
Kramer, C., Alves, J., Lada, C. J., Lada, E. A., Sievers, A., Ungerechts, H., & Walmsley, M. 1999, A&A, 342, 257
Kuiper, T. B. H., Langer, W. D., & Velusamy, T. 1996, ApJ, 468, 761
Lacy, J. H., Knacke, R., Geballe, T. R., & Tokunaga, A. 1994, ApJ, 428, L69
Léger, A., Jura, M., & Omont, A. 1985, A&A, 144, 147
Lehtinen, K., Lemke, D., Mattila, K., & Haikala, L. K. 1998, A&A, 333, 702
Lemme, C., Wilson, T. L., Tieftrunk, A. R., & Henkel, C. 1996, A&A, 312, 585

Linke, R. A., Goldsmith, P. F., Wannier, P. G., Wilson, R. W., & Penzias, A. A. 1977, ApJ, 214, 50
Mathis, J. S., Mezger, P. G., & Panagia, N. 1983, A&A, 128, 212
Mauersberger, R., Wilson, T. L., Mezger, P. G., Gaume, R., & Johston, K. 1992, A&A, 256, 640
Nelson, R. P., & Langer, W. D. 1997, ApJ, 482, 796
Neufeld, D. A., & Kaufman, M. J. 1993, ApJ, 418, 263
Neufeld, D. A., Lepp, S., & Melnick, G. J. 1995, ApJS, 100, 132
Neufeld, D. A., Melnick, G. J., & Harwit, M. 1998, ApJ, 506, L75
Ohashi, N., Lee, S. W., Wilner, D. J., & Hayashi, M. 1999, ApJ, 518, L41
Ohishi, M., Irvine, W. M., & Kaifu, N. 1992, in IAU Symp. 150, Astrochemistry of Cosmic Phenomena, ed. P. D. Singh (Dordrecht: Kluwer), 171
Phillips, T. R., Maluendes, S., & Green, S. 1996, ApJS, 107, 467
Preibisch, Th., Ossenkopf, V., Yorke, H. W., & Henning, Th. 1993, A&A, 279, 577
Schilke, P., Keene, J., LeBourlot, J., Pineau des Forêts, G., & Roueff, E. 1995, A&A, 294, L17
Schinke, R., Engel, V., Buck, U., Meyer, H., & Diercksen, G. H. F. 1985, ApJ, 299, 939
Schröder, K., Staemmler, V., Smith, M. D., Flower, D., & Jaquet, R. 1991, J. Phys. B, 24, 2487
Snell, R. L., et al. 2000a, ApJ, 539, L93
———. 2000b, ApJ, 539, L97
———. 2000c, ApJ, 539, L101
Tielens, A. G. G. M., & Whittet, D. C. B. 1997, in IAU Symp. 178, Molecules in Astrophysics: Probes and Processes, ed. E. F. van Dishoeck (Dordrecht: Kluwer), 45
Turner, B. E., Chan, K.-W., Green, S., & Lubowich, D. A. 1992, ApJ, 399, 114
van Dishoeck, E. F., & Black, J. H. 1986, ApJS, 62, 109
Visser, A. E., Richer, J. S., Chandler, C. J., & Padman, R. 1998, MNRAS, 301, 585
Werner, M. W., & Salpeter, E. E. 1969, MNRAS, 145, 249
Willacy, K., Klahr, H. H., Millar, T. J., & Henning, Th. 1998a, A&A, 338, 995
Willacy, K., Langer, W. D., & Velusamy, T. 1998b, ApJ, 507, L171
Willacy, K., & Williams, D. A. 1993, MNRAS, 260, 635
Wilner, D. J., Myers, P. C., Mardones, D., & Tafalla, M. 2000, ApJ, 544, L69